Effects of Ru on the High-Temperature Phase Stability of Ni-Base Single-Crystal Superalloys

A.C. YEH and S. TIN

Microstructural instabilities associated with the precipitation of refractory-rich topologically-close-packed (TCP) phases within the microstructure of advanced Ni-base single-crystal superalloys were quantified in two nominally identical alloys with and without additions of Ru. Differences in the microstructural kinetics associated with the formation of TCP precipitates in these experimental single-crystal superalloys enabled the influence of Ru to be assessed. Detailed microstructural investigations were carried out on specimens subjected to prolonged isothermal exposures at elevated temperature. Even after 1000 hours at temperatures in excess of 1100 °C, the microstructure of the Ru-bearing alloy was highly resistant to the formation of TCP phases. Transmission electron microanalysis (TEM) coupled with X-ray diffraction (XRD) was used to identify the characteristic crystal structures of the TCP precipitates in both alloys as being primarily the orthorhombic P and tetragonal σ phase. The sluggish precipitation kinetics of TCP phases in the Ru-bearing single-crystal Ni-base superalloy prevents the breakdown of the parent γ-γ' microstructure and greatly enhances the high-temperature creep characteristics.

I. INTRODUCTION

RECENT trends in the development of high-temperature structural materials for the gas turbine for aerospace applications have focused on the addition of increasingly high levels of refractory elements, such as Re and W, to single-crystal Ni-base superalloys.[1–5] These elemental additions are extremely potent in enhancing the strength and creep performance of the alloy at low to intermediate temperatures (750 °C to 950 °C). At elevated temperatures (>1000 °C), however, W and Re additions tend to promote microstructural instabilities that lead to the rapid formation of refractory-rich topologically-close-packed (TCP) precipitates.[1,4,6–9] Precipitation of these deleterious phases removes the refractory solid solution strengthening elements from the constituent γ-γ' phases. Consequently, creep properties have been shown to degrade rapidly as TCP formation occurs within the microstructure.[10,11] Since single-crystal Ni-base superalloy turbine blades are required to operate under a range of temperatures and stresses, the composition of the alloy has to be carefully engineered to provide a balanced set of properties. In many advanced high refractory content Ni-base superalloys, the microstructural instabilities occurring at elevated temperature severely limit the degree to which W and Re additions can be used to improve the low and intermediate temperature creep properties.

Superalloys are engineering materials that often contain in excess of ten alloying additions. Due to the complex chemistries, predicting element interactions and the formation of equilibrium phases in this class of alloys is challenging. Furthermore, due to the low diffusivities of tungsten and rhenium in nickel at elevated temperatures, precipitation reactions involving these elements become sluggish and phases may precipitate as isolated plates or discontinuously with cellular morphologies.[6,7,9,10,12] The variety of TCP phases that may potentially form in Ni-base superalloys (P, μ, R, and σ) are typically characterized by close-packed layers of atoms forming "basketweave" sheets, which are often aligned with the octahedral planes in the fcc matrix. Similarities in the composition and crystallography of the TCP phases enables these precipitates to develop as mixed structures consisting of a number of different phases.[6,7,8] Although the chemistries of the TCP phases are dependent upon the composition of the parent alloy, these phases can be distinguished by their distinct crystallographic structures (Table I). The μ- and R-phase precipitates have a rhombohedral crystal structure, while the σ phase is tetragonal and the P phase is orthorhombic.

Recent studies have shown that additions of the platinum group metal, Ru, can potentially be used to suppress the formation of TCP phases in Ni-base superalloys.[2,3,5,11] Alloys containing additions of Ru were shown to exhibit significantly improved high-temperature creep properties since the absence of the TCP phases enabled the refractory alloying additions to remain within the γ-γ' phases and provide a high degree of solid solution strengthening.[11,13] This characteristic attribute of Ru additions in Ni-base superalloys enables higher overall levels of refractory elements to be accommodated within the alloy to enhance low- to intermediate-temperature creep strength.

Initial efforts to elucidate the effect of Ru described a corresponding change in chemical partitioning between the γ and γ' phases.[14] Changes in the partitioning characteristics of the constituent elements due to the presence of Ru were shown to decrease the degree of Re supersaturation in the γ phase and to lower the susceptibility of the alloy for TCP precipitation. However, recent atom probe tomography studies on two nominally identical alloys with and without Ru revealed no significant changes in partitioning

A.C. YEH, formerly Graduate Researcher, Rolls-Royce University Technology Partnership Materials Science and Metallurgy Department, University of Cambridge, Cambridge CB2 3QZ, United Kingdom, is Postdoctoral Researcher, The National Institute of Materials Science, Tskuba 305-0047, Japan. S. TIN, formerly Assistant Director of Research, Rolls-Royce University Technology Partnership Materials Science and Metallurgy Department, University of Cambridge, is Associate Professor, Illinois Institute of Technology, Chicago, IL 60616. Contact e-mail: tin@iit.edu

Manuscript submitted January 24, 2006.

characteristics associated with the presence of Ru.[15,16] Partitioning measurements in other experimental single-crystal Ni-base superalloys using transmission electron microscopy–energy-dispersive spectroscopy (TEM-EDS)[17] and wavelength-dispersive spectroscopy (WDS)[18] also indicated minimal changes in chemical partitioning attributed to the presence of Ru additions.

The fundamental mechanisms by which Ru additions are able to improve the high-temperature phase stability of Ni-base superalloys are still unclear. In order to further optimize the physical and mechanical properties of these advanced Ni-based superalloys, a detailed understanding of the effects associated with Ru is required. In this study, the influence of Ru on the phase stability of experimental high refractory content Ni-base single-crystal superalloys was investigated. Evidence suggesting that the Ru additions inhibit the growth kinetics of TCP phases during extended isothermal exposures is presented and the implications of these results are discussed.

II. EXPERIMENTAL MATERIALS AND PROCEDURES

Single-crystal bars of alloys RR2100 and RR2101 were directionally solidified using investment molds at the Rolls-Royce plc precision casting foundry located in Derby, United Kingdom. Compositions of the experimental single-crystal alloys are listed in Table II. Alloy RR2101 is nominally identical to RR2100 with the exception of the 2 wt pct Ru addition, which was substituted for nickel. After solidification, the single-crystal bars measuring 12.7 mm in diameter and 150 mm in length were solution heat treated to minimize chemical heterogeneities within the microstructure due to dendritic segregation using the standard CMSX-10 solution treatment. This heat treatment was comprised of a long, ramped cycle rising in steps to 1364 °C, at which temperature the material was held for 20 hours. Postsolutioning, the alloys were subjected to a primary age of 5 hours at 1140 °C and secondary age of 16 hours at 870 °C.

Electron probe microanalysis was used to assess the degree of residual segregation present in the microstructures of the two alloys after the solution and aging treatments. A Cameca (Paris, France) SX50 electron probe microanalyzer equipped with thallium acid phthalate (for Al, Ta, Re), lithium fluoride (for Cr, Co, Ni), and pentaerythritol (for W and Ru) diffracting crystals was used for quantitative segregation analysis[19,20] using WDS. A series of discrete compositional point measurements were taken over a representative area of the microstructure (1 mm × 1 mm). Coupled with a dwell time of 75 seconds per point, a 20-kV accelerating voltage and a 100-nA beam current were found to yield the most accurate results.

Specimens were sectioned from the solution-heat-treated RR2100 and RR2101 single crystals and carefully prepared for the isothermal exposures. To minimize oxidation, the specimens were sealed in silica tubes and flushed with argon. A range of exposure temperatures and times (up to 1180 °C and 2000 hours, respectively) were investigated to assess the kinetics of TCP precipitation. Following the isothermal exposures, experiments were carried out to investigate the effect of Ru on the formation of TCP precipitates.

Microstructures of the solution-heat-treated RR2100 and RR2101 specimens before and after the elevated temperature exposures were observed using a JEOL* 5800LV scanning electron microscope equipped with an electron backscatter detector. Prior to examination, samples were prepared using standard metallographic techniques and a final polish of colloidal silica. The general purpose etching solution for the single-crystal superalloy—Nimonic (80 mL HCL, 20 mL H_2O, 2 mL HNO_3, and 16 g $FeCl_3$)—was used to reveal the microstructures. The volume fraction and distribution of TCP phases corresponding to different exposure times and temperatures were quantified using image analysis software.

*JEOL is a trademark of Japan Electron Optics Ltd., Tokyo.

For TEM analysis, the isothermally aged specimens were sectioned along the {111} planes of the single crystals to obtain low index orientations that enable analysis of the characteristic TCP diffraction patterns. Two foil preparation techniques were used to prepare the thin disks (~3 mm in diameter and 0.4 mm in thickness) for TEM analysis. Depending on the type of analysis required, either ion beam milling or electrolytic thinning was used to process the TEM specimens. Disk-shaped foils were mechanically ground to

Table I. Basic Crystallography of the σ, μ, P, and R phases

Phase	Typical Example	Unit Cell	Atoms per Cell*	a (Å)**	b (Å)**	c (Å)**
σ	$Cr_{46}Fe_{54}$	tetragonal	30	8.8	—	4.544
μ	Mo_6Co_7	rhombohedral	39	4.762	—	25.61
P	$Cr_{18}Mo_{42}Ni_{40}$	orthorhombic	56	9.07	16.98	4.752
R	$Cr_{18}M0_{31}Co_{51}$	rhombohedral	159	10.9	—	19.54

*The lattice parameters of μ and R phases are defined on hexagonal axes.
**Based on primary rhombohedral cell.

Table II. Nominal Chemical Compositions of RR2100 and RR2101 (Weight Percent)

Alloy	Co	Cr	W	Re	Ru	Al	Ta	Ni
RR2100	12.0	2.5	9.0	6.4	—	6.0	5.5	bal
RR2101	12.0	2.5	9.0	6.4	2.0	6.0	5.5	bal

~0.1 mm in thickness, and electrochemically thinned using a twin-jet polisher with a solution of 10 pct perchloric acid in methanol between −2 °C and −3 °C for RR2100 and −5 °C and −7 °C for RR2101. For electron diffraction studies and quantitative chemical analyses of TCP precipitates, ion beam milling techniques were applied to ensure uniform thinning of the embedded TCP phases. Sample preparation involved first thinning the disk to ~50 μm using the twin-jet polisher under the same conditions as described previously, and then using a Gatan (Warrendale, PA) precision ion polishing system (PIPS-Model 691) for final thinning. During the process, the sample was axially rotated and ion milled on both sides with Ar ions under high vacuum (~5×10^{-5} Torr), with 5 kV accelerating voltage and 10 deg ion gun angle. After perforation, the accelerating voltage was reduced to 2 kV to remove ion beam damage. A JEOL 2000FX TEM was used to characterize TCP phases using selected area diffraction (SAD). A FEI Tecnai (Eindhoven, Netherlands) F20 TEM equipped with an EDS system was used to determine the chemical composition of the TCP phases. The reported results were based on a minimum of five TEM samples for every condition to ensure a representative microstructure was analyzed.

The TCP precipitates were also extracted from the isothermally aged specimens for phase identification using X-ray diffraction (XRD). Specimens were immersed in an electrolyte composed of 10 pct HCl and 1 pct tartaric acid in methanol with an anodic current density of 2 mA/mm^2 at room temperature for 8 hours. Residue consisting of the extracted TCP phases was carefully collected and analyzed. A PHILIPS* PW1050 system with a calibrated vertical diffractometer, and Cu K_α radiation was used to perform XRD analysis on the extracted precipitates. The detector range was set between 20 and 100 deg for 2θ values with step size 0.05 deg for RR2100 and 0.02 deg for RR2101; acquisition time per step was 2 seconds for RR2100 and 5 seconds for RR2101. The resulting diffraction patterns were processed using PHILIPS X'Pert software to determine peak positions and compare with the JCPDS-ICDD reference database.

*PHILIPS is a trademark of Philips Electronic Instruments Corp., Mahwah, NJ.

Precipitation of TCP phases in polycrystalline specimens of RR2100 and RR2101 was also investigated in an effort to quantify the effects of Ru additions on the growth kinetics. Unlike single crystals that typically possess a large nucleation barrier, polycrystalline specimens are much more prone to TCP formation as these intermetallic phases are able to nucleate readily along high-angle grain boundaries. Single-crystal samples of solution-heat-treated RR2100 and RR2101 were deliberately recrystallized by locally deforming the microstructure with a Vickers hardness indenter. Following deformation, the samples were sealed in a silica tube with Ar gas and annealed at 1285 °C for 1 hour to promote recrystallization. The recrystallized microstructures were then subjected to isothermal exposures at 1180 °C for 1.5, 10, and 100 hours. Growth rates of the TCP phases developing along grain boundaries with similar misorientations in both alloys were compared. Electron backscatter diffraction (EBSD) was used to measure grain boundary misorientations in the polycrystalline specimens and to correlate the results with the observed TCP growth rates for both alloys.

III. RESULTS AND ANALYSIS

Due to the elevated level of refractory alloying additions, the microstructure of alloy RR2100 was revealed to be an inherently unstable alloy with respect to the formation of TCP phases. The presence of isolated TCP phases was observed immediately after the secondary aging treatment and prior to the isothermal exposures in alloy RR2100 (Figure 1(a)). No TCP phases were present in the

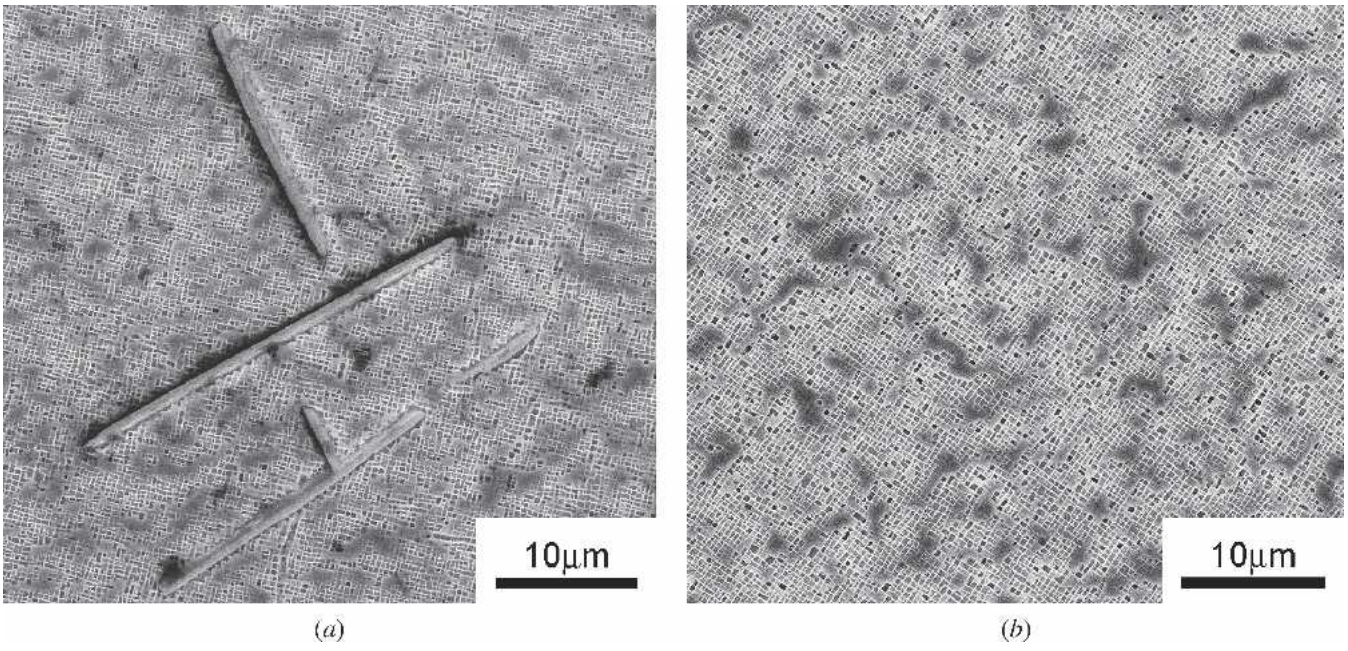

Fig. 1—Microstructures of (*a*) RR2100 and (*b*) RR2101 after the initial solution and primary aging heat treatments. Local precipitation of TCP phases occurred within the dendritic region alloy RR2100 prior to the isothermal exposures.

microstructure of the Ru containing alloy, RR2101, until after a prolonged exposure at elevated temperature. For both alloys, the degree of residual segregation measured in the starting microstructure was extremely low. The only elements that showed any significant degree of residual segregation were Re and Ta, which varied from 6.5 to 4.5 wt pct and 5.0 to 6.0 wt pct, respectively, between the dendritic and interdendritic regions. Despite the presence of Ru in alloy RR2101, no major differences in chemical heterogeneity were detected in the microstructure after the solution and aging treatments.

Comparison of the microstructural stability of the two alloys at 1100 °C reveals substantial differences in the kinetics associated with the precipitation of TCP phases

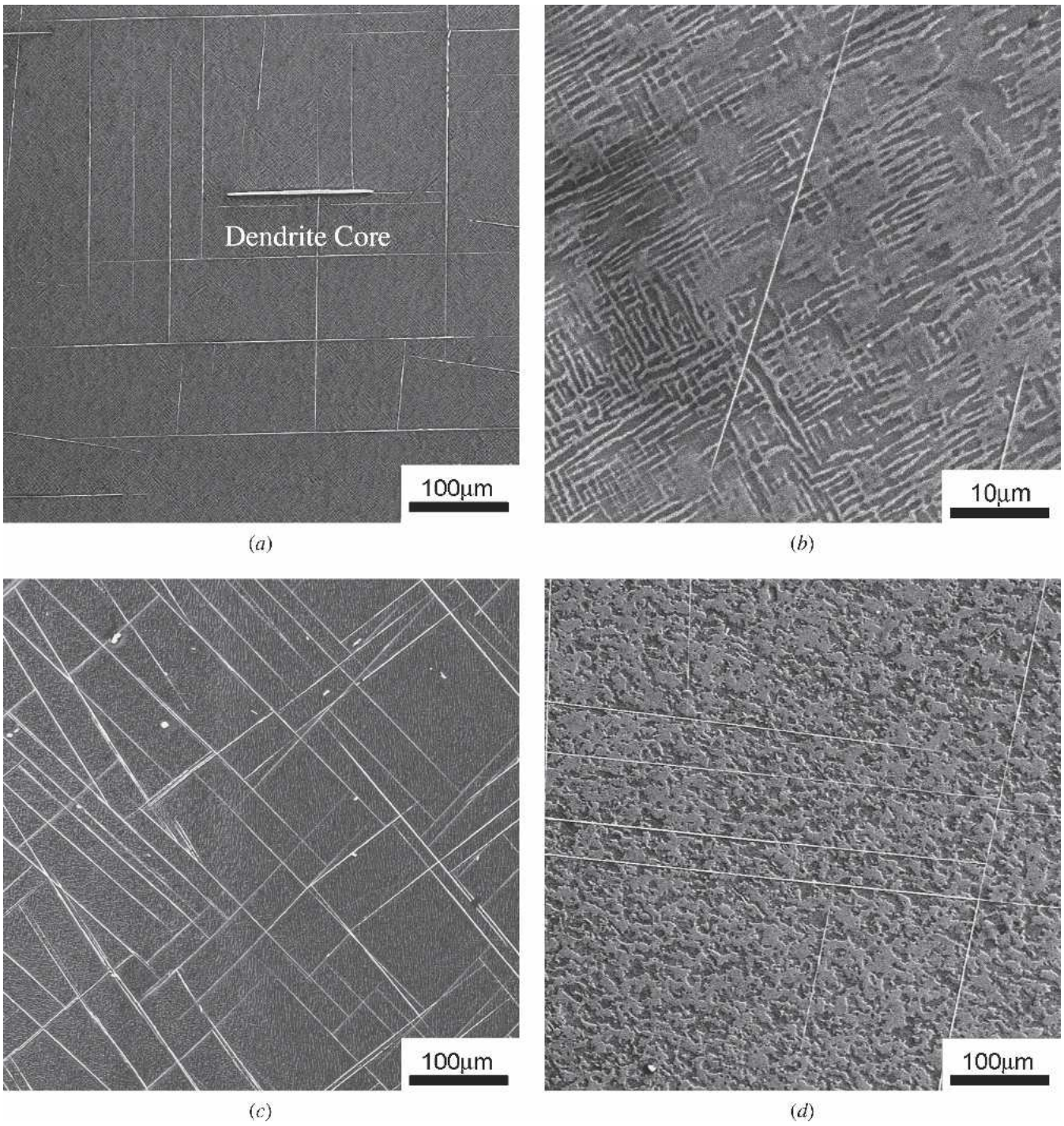

Fig. 2—Representative microstructures of RR2100 after (*a*) 100 h and (*c*) 1000 h at 1100 °C. Initially, the TCP phases precipitate locally within the dendrite core in RR2100 and gradually percolate into the interdendritic regions upon further exposure to elevated temperature. In alloy RR2101, the onset of TCP precipitation within the dendrite core occurred after (*b*) 400 h at 1100 °C. Although TCP phases could be observed throughout the microstructure in RR2101 (*d*) after 2000 h at 1100 °C, the morphology of the precipitates remained extremely fine.

(Figure 2). Although the presence of TCP precipitates prior to the isothermal exposures in RR2100 may have possibly enhanced the precipitation of TCP phases by providing nucleation sites at the dendrite cores, this does not account for the sluggish growth of TCP precipitates in RR2101. In both alloys, the TCP precipitates first form at regions associated with the dendrite core and eventually spread into interdendritic regions and cover the entire microstructure. The rate at which these TCP phases formed in the alloys was significantly influenced by the presence of Ru. In alloy RR2100, coarse, blocky TCP phases were initially present in the dendritic regions of the microstructure in the as-solutioned condition prior to the isothermal exposures. These initial TCP precipitates are easily distinguishable from the TCP precipitates forming during the isothermal exposure due to their coarse features and preferential location within the microstructure. After 100 hours at 1100 °C, TCP precipitates in alloy RR2100 continued to form, but were primarily confined within the dendritic regions of the microstructure (Figure 2(a)). The TCP phases were present throughout the entire microstructure in RR2100 after 1000 hours at 1100 °C (Figure 2(c)). For the Ru-containing alloy, RR2101, small traces of TCP phases were observed within the dendrite cores only after 400 hours at 1100 °C (Figure 2(b)). The growth rate of these TCP phases in RR2101 was extremely sluggish, because they were still mainly confined within the dendritic regions of the microstructure after 1000 hours. Only after 2000 hours at 1100 °C were TCP precipitates observed throughout the microstructure (Figure 2(d)). The precipitate morphologies, however, were rather unique, because they remained extremely fine and comprised a much smaller area fraction when compared to the TCP precipitates in RR2100 after 1000 hours.

Figure 3 provides a schematic illustration of the microstructural changes occurring during isothermal aging of RR2100 and RR2101 at 1100 °C. Stage I corresponds to the initial formation of TCP precipitates at the dendrite core. These regions of the microstructure are associated with moderate to high degrees of residual Re segregation. As precipitation of the TCP phases progresses, they begin to form preferentially within the remaining dendritic regions of the microstructure, stage II, prior to infiltrating out into the interdendritic regions, stage III. Continued isothermal exposure results in uniform growth of the precipitates until the equilibrium volume fractions of the constituent phases are reached. Comparison of the results at 1100 °C reveals that it took approximately twice as long for RR2101 to reach stage III than it did RR2100.

Observations of the microstructural changes occurring at the TCP and matrix interfaces in both RR2100 and RR2101 were also made to better understand how the Ru additions were contributing to the improved phase stability at elevated temperatures. Specimens for both alloys were carefully selected such that the TCP phases analyzed both formed during the isothermal exposure and not during the initial solution heat treatment or primary aging treatment. Growth of the TCP phases in RR2100 led to the formation of a γ' envelope surrounding the precipitate after 100 hours at 1100 °C (Figure 4(a)). Coinciding with the coarsening of the γ-γ' microstructure away from the TCP phases, continued growth of the TCP phase during an isothermal exposure of 1000 hours resulted in thickening of the γ' envelope (Figure 4(c)). Compared to RR2100, the microstructural transformations occurring at the interfaces of the TCP phases in RR2101 were extremely sluggish. Even after 1000 hours at 1100 °C, only a limited amount of coarsening of the γ/γ' matrix occurred around TCP phases (Figure 4(b)). Unlike the TCP precipitates in RR2100, which were embedded within an envelope γ' after only 100 hours at temperature, TCP precipitates in RR2101 were observed to reside adjacent to both γ and γ' phases even after 1000 hours at 1100 °C. Dissolution of the γ phase around the TCP precipitates and formation of the γ' envelope in RR2101 did not occur until approximately 2000 hours at 1100 °C (Figure 4(d)).

As the bulk microstructure continues to change with longer aging times, localized microstructural changes also occur in regions adjacent to the TCP phases. Figure 5 presents a schematic showing three distinct stages of TCP growth. After the TCP phases nucleate, the precipitate is embedded within a matrix consisting of both γ and γ' phases, stage A. Continued growth of the TCP phase results in a gradual depletion of the refractory alloying additions in the γ phase and causes dissolution of the γ phase surrounding the precipitate, stage B. Eventually, the growing TCP precipitate consumes all of the refractory elements in the

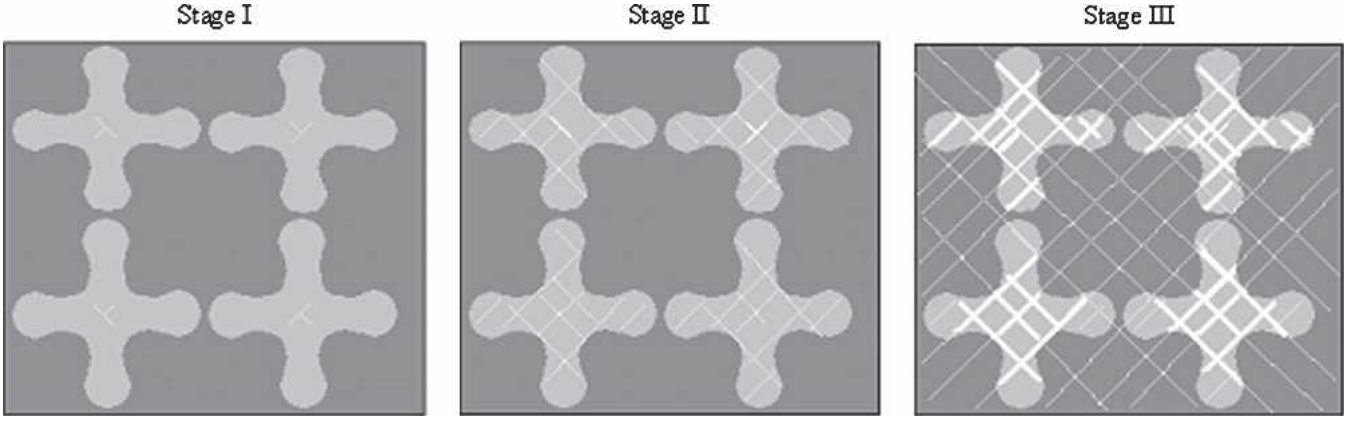

Fig. 3—Schematic illustration of the sequence of TCP precipitation in single-crystal Ni-base superalloys. The TCP phases initially form within the dendritic cores of the microstructures and gradually spread into the interdendritic regions.

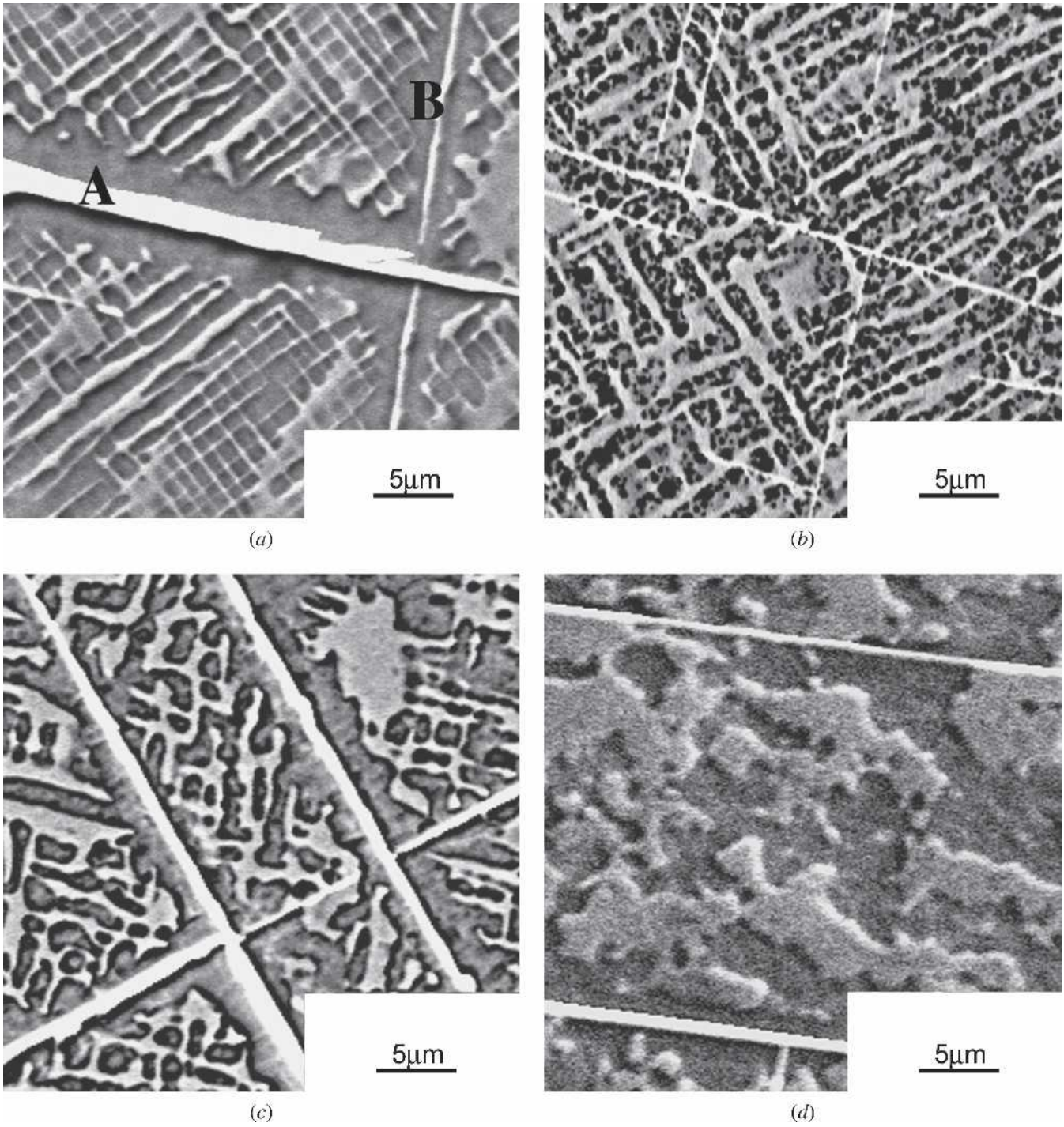

Fig. 4—Micrographs showing localized changes in the microstructure adjacent to the TCP after isothermal exposures. (*a*) After 100 h at 1100 °C, an envelope of γ' had formed around the TCP precipitates in alloy RR2100. The coarse TCP precipitate, *A*, was present in the microstructure prior to the thermal exposure, while the fine TCP precipitate, *B*, formed during the exposure. (*c*) Coarsening of the fine TCP precipitates in alloy RR2100, *B*, occurred after 1000 hours at 1100 °C and coincided with thickening of the surrounding γ' envelope. Despite a (*b*) 1000 h and (*d*) 2000 h isothermal exposure at 1100 °C, limited coarsening of the TCP phases in alloy RR2101 was observed.

γ phase and becomes embedded within an envelope of γ', stage C. Should the TCP precipitates continue to coarsen, the envelope of γ' also becomes thicker until local equilibrium conditions are achieved. In RR2100, TCP precipitates were able to reach stage C after only 100 hours, while it took over 2000 hours at 1100 °C for the TCP precipitates in RR2101 to attain stage B. The presence of the 2 wt pct Ru in RR2101 clearly influences the microstructural transformations at this temperature and appears to reduce the growth kinetics of the reaction by a factor of approximately ~20.

The isothermal exposures indicate that the Ru additions strongly reduce the kinetics of the microstructural transformations at elevated temperatures and suppress the formation

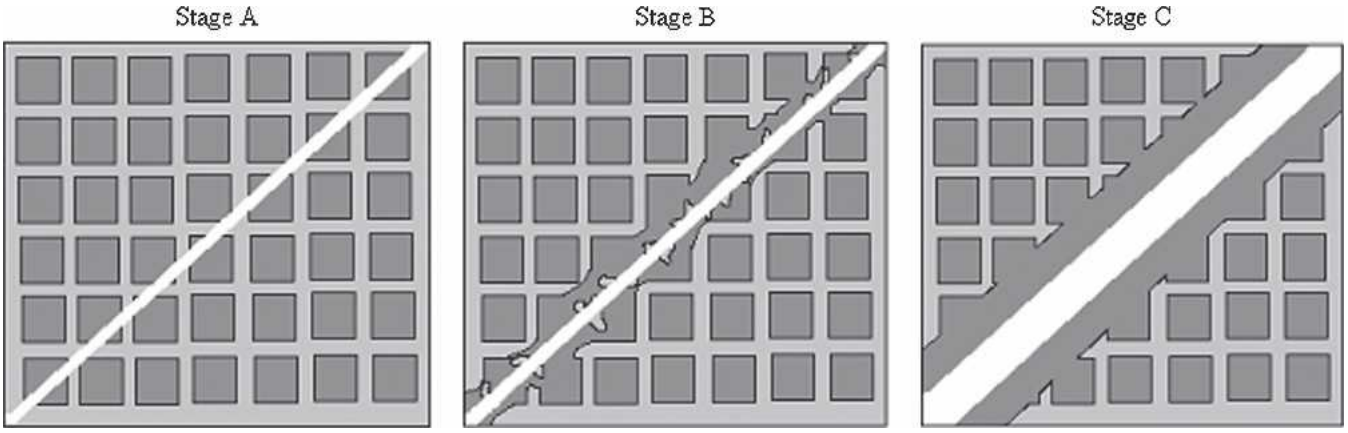

Fig. 5—Schematic illustration revealing the sequence of local microstructural changes occurring adjacent to the TCP precipitates.

of TCP phases. Changes in the nucleation characteristics in these two experimental single-crystal alloys were also investigated using polycrystalline specimens of RR2100 and RR2101 subjected to isothermal exposures at 1180 °C for various durations. The presence of high-angle grain boundaries provides a large number of heterogeneous nucleation sites and enables effective comparison of the growth kinetics associated with TCP precipitation. The formation of TCP phases along similarly misoriented grain boundaries in the two alloys is presented in Figures 6(a) and (b). Misorientation angles between adjacent grains were measured to be between 42 and 44 deg using standard EBSD techniques. For both alloys, TCP phases were first observed along the high-angle boundaries after only 90 minutes. The size, area fraction, and morphology of the TCP precipitates appear to be similar for both alloys. Prolonged exposure of these polycrystalline specimens resulted in cellular precipitation and the formation of colonies consisting of γ and TCP lamellae contained within a γ' matrix. Along highly misoriented boundaries (~42 to 44 deg), the average fractions of the constituent phases comprising the colonies are very similar even after thermal exposures of 10 and 100 hours at 1180 °C (Figures 6(c) through (f)).

Detailed analysis of the TCP phases in the isothermally exposed single-crystal specimens was carried out to characterize possible differences in chemical composition or crystal structure associated with the presence of Ru. For analysis in the TEM, rapid formation of TCP phases was induced throughout the microstructure in the single crystals by subjecting the specimens to an isothermal exposure at 1180 °C. Samples of RR2100 were annealed for 150 hours while the more stable specimens of RR2101 were annealed for 320 hours to generate a sufficiently dense population of TCP precipitates for examination in the TEM. The SAD patterns were used to identify the characteristic crystal structures of the TCP phases present in the two alloys. Figure 7(a) shows that both P phase and σ phase were present in alloy RR2100. Although the chemical compositions of the two phases were extremely similar, the majority of the precipitates analyzed in RR2100 were P phase. Table III shows the high levels of Re and W content measured in both precipitates. Despite the longer isothermal exposure, significantly fewer TCP precipitates were present in RR2101. Consistent with RR2100, the majority of the TCP phases in RR2101 were identified to possess the orthorhombic crystal structure characteristic of the P phase (Figure 7(b)). Identification of TCP phases was also confirmed *via* X-ray scans of the extracted precipitates. The *P*- and σ-phase precipitates were present in both of the single-crystal alloys after a prolonged thermal exposure; however, the proportion of P phase precipitates was determined to be much higher for both RR2100 and RR2101. Interestingly, compositional analysis of the TCP phases in RR2101 revealed that the chemistries of the *P*- and σ-phase precipitates in both RR2100 and RR2101 were nearly identical as Ru was noticeably absent within the TCP phase of RR2101 (Table III).

The effects of Ru on the variation in γ' volume fraction as a function of temperature was also investigated. For both of the experimental alloys, specimens were held isothermally at various temperatures ranging from 900 °C to 1100 °C prior to being rapidly quenched to room temperature in order to retain microstructures representative of those at temperature. Hold times of 4 hours were used to minimize the effects of TCP precipitation in RR2100 and to yield consistent results. By calculating the overall fraction of primary γ' precipitates observed within the microstructure, the equilibrium volume fraction of γ' was estimated as a function of temperature. Although the fraction of γ' in both alloys was measured to be nominally identical at room temperature, substantial differences in microstructure were observed between the two alloys at 1000 °C and 1100 °C (Table IV). The Ru-bearing alloy, RR2101, was observed to contain 5.3 and 10.2 pct less γ' than alloy RR2100 at 1000 °C and 1100 °C, respectively.

IV. DISCUSSION

In advanced single-crystal Ni-base superalloys, refractory elements used to enhance high-temperature strength, such as rhenium and tungsten, tend to segregate heavily to the dendrite core during solidification.[19,21–23] This characteristic partitioning behavior during dendritic solidification leads to a supersaturation of tungsten and rhenium at the dendrite core in the as-cast structure. Despite lengthy solutioning treatments at elevated temperature, moderate levels of residual segregation still occur within the dendritic microstructure (Figure 1). Compositional differences within the dendritic structure combined with the elevated levels of

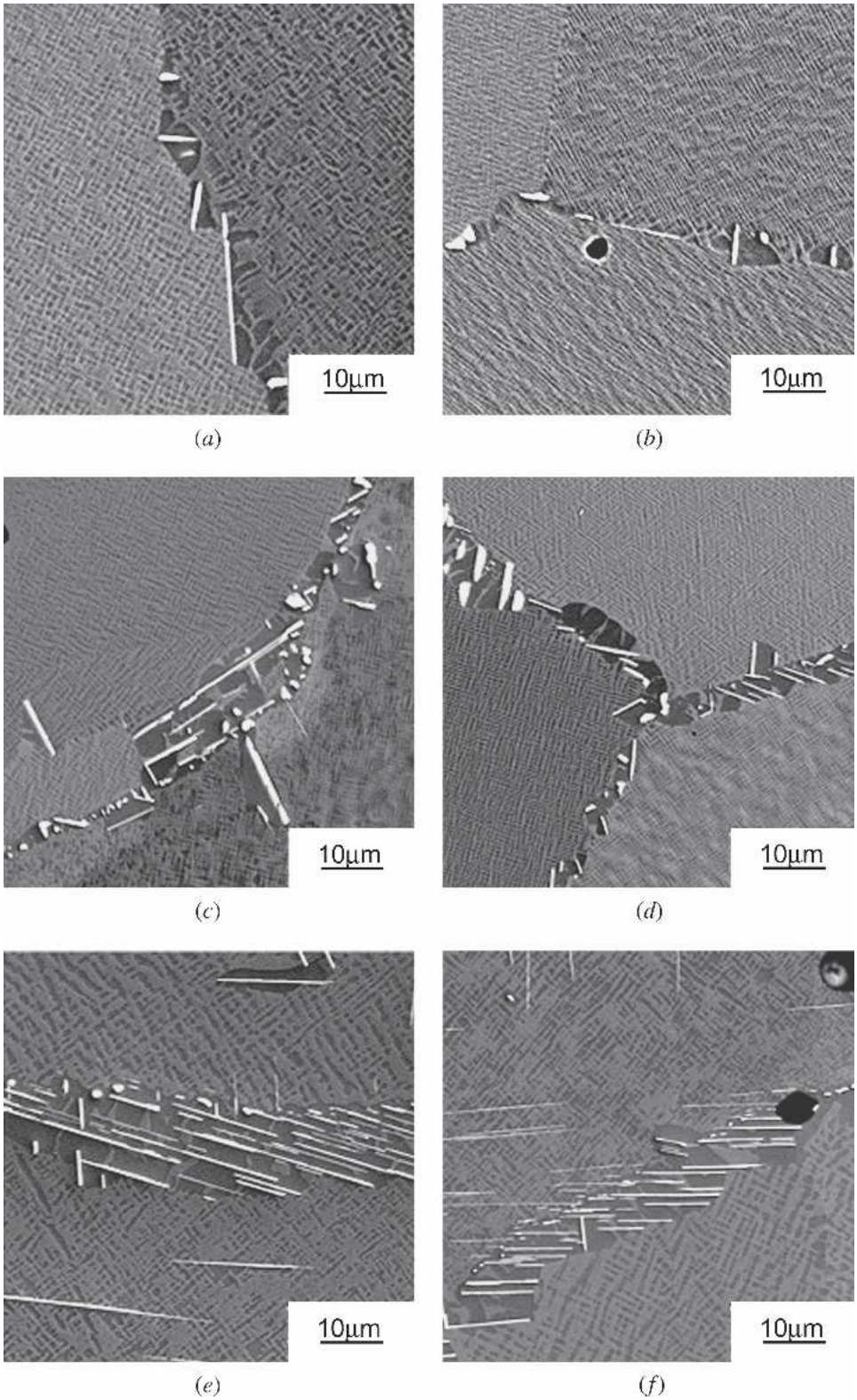

Fig. 6—Micrographs depicting cellular precipitation along high-angle grain boundaries. In all instances ((*a*) through (*f*)), grain boundary misorientations were measured to be between 42 and 44 deg. In both (a) RR2100 and (b) RR2101, discontinuous cellular precipitation of TCP phases occurred after only 90 min at 1180 °C. The interfaces of the cellular precipitates were comparatively mobile as significant growth occurred in alloy RR2100 after (*c*) 10 h and (*e*) 100 h at 1180 °C, respectively. The cellular precipitates observed in RR2101 were also noted to consist of moderate levels of TCP lamellae after (*d*) 10 h and (*f*) 100 h at 1180 °C.

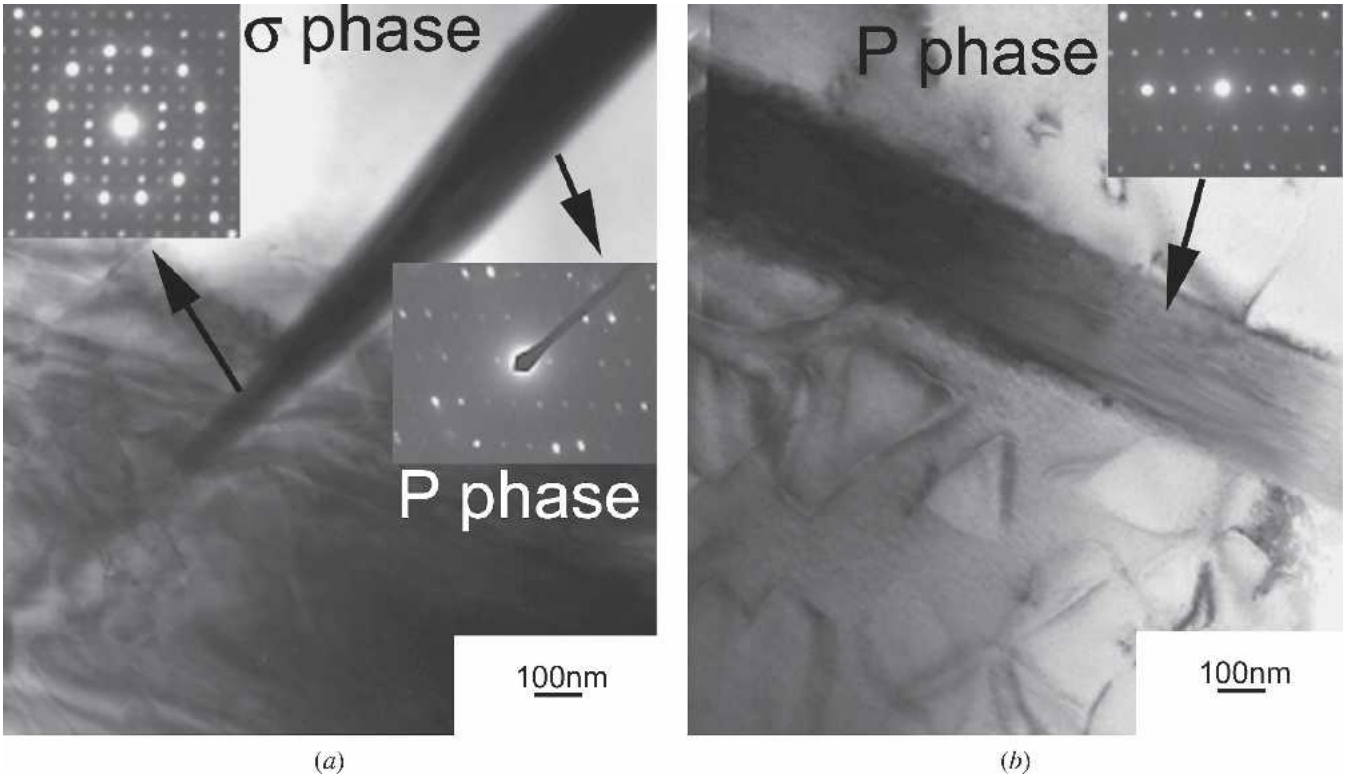

Fig. 7—TEM micrographs and diffraction patterns associated with the TCP phases in (*a*) RR2100 and (*b*) RR2101.

Table III. Compositions of the TCP Phases in Alloys RR2100 and RR2101 Determined Using TEM/EDS (Weight Percent); Measurement Errors for Al, Cr, Co, Ni, Ru, and Ta are <0.2 pct, While the Errors for W and Re are <1.0 pct

Alloy	Phase	Al	Cr	Co	Ni	Ru	Ta	W	Re
RR2100	σ	0.8	1.8	4.4	7.4	—	0	28.9	55.6
RR2100	*P*	1.2	2.1	4.5	6.9	—	0	28.0	57.0
RR2101	σ	0.9	1.5	5.2	8.3	0	0	27.3	55.2
RR2101	*P*	0.9	1.1	4.6	5.4	0	0	28.0	59.0

Re and W present within the γ phase ultimately lead to the formation of intermetallic TCP phases after prolonged exposure to elevated temperatures. In addition to gradually depleting the microstructure of W and Re, precipitation and growth of TCP phases at elevated temperatures also coincides with morphological changes in the γ-γ' microstructure (Figures 2 and 4). Although the experimental results clearly demonstrate that Ru additions can be effectively used to minimize the occurrence of these deleterious precipitates at elevated temperatures, the manner in which Ru additions affect the underlying mechanisms associated with TCP precipitation is not clear. Previous studies have attributed a lesser degree of refractory element supersaturation in the γ phase of Ru-bearing Ni-base superalloys.[14] Since detailed compositional analyses did not provide evidence of changes in chemical partitioning between the γ and γ' phases for this particular set of experimental alloys,[15,16] the role of Ru on the nucleation and growth kinetics of TCP phases is worth considering. This is especially important as a number of other studies have also reported minimal changes in partitioning due to the addition of Ru.[17,18] Because the various TCP phases were observed to exhibit specific orientation relationships with the γ-γ' microstructure, nucleation of precipitates occurred along specific crystallographic planes.[6–8] The presence of Ru in the γ phase and the resulting change in lattice misfit between the γ phase and TCP may potentially influence the ability of the TCP phases to nucleate. Furthermore, because Ru was not detected within the TCP phases, the presence of this particular platinum group element may alter some aspect of the TCP coarsening kinetics. Each of these possibilities is considered here in light of the experiments conducted in this study.

One possible mechanism by which Ru additions enhance phase stability can be related to the degree of segregation during unidirectional solidification. The driving force for precipitation of TCP phases can be minimized by controlling the degree of tungsten and rhenium segregation and preventing the dendrite cores from becoming supersaturated with refractory solute. Although the extent to which Re, W, and Ta are segregated in the as-cast dendritic microstructure was measurably lower in the Ru-bearing alloy, RR2101, the lengthy solution heat treatment assisted in normalizing the compositional heterogeneities prior to the isothermal exposures. Despite a nearly identical level of residual segregation in both single-crystal alloys, RR2100 exhibited a much higher tendency to form TCP phases during the subsequent thermal exposures. Clearly, the microstructural stability of RR2101 can be attributed to the presence of Ru within the constituent γ-γ' phases.

Compared to the fcc γ and $L1_2$ ordered γ' lattice, the crystal structures associated with the TCP phases are extremely complex. Often comprised of hundreds of atoms, the size of the unit cell associated with the TCP phases is significantly larger than the lattice of the γ and γ' phases. Consequently, a large nucleation barrier serves to prevent the formation of these undesirable phases in the microstructures of single-crystal Ni-base superalloys. When TCP phases do eventually form in these alloys, they nucleate preferentially on close-packed planes, forming a semicoherent interface, and exhibit distinctive orientation relationships with the parent crystal.[6–8] Following nucleation, growth of the TCP precipitates is highly anisotropic as the interfacial conditions surrounding the precipitates vary considerably. While the semicoherent interfaces are restricted to growing *via* a ledge-type mechanism, the incoherent ends of the precipitate are comparatively mobile and migration is primarily limited by diffusion. Similar to intermetallic precipitates in a wide range of multicomponent alloy systems, the growth anisotropy of σ- and *P*-phase precipitates leads to the formation of rod- or platelike morphologies observed in these single-crystal superalloys. High-resolution TEM and lattice imaging results at the TCP/γ-γ' matrix of similar alloys[24] have shown that, although the presence of Ru does slightly modify the density of growth ledges, the changes are relatively minor and do not account entirely for the differences in microstructural stability between alloys with and without additions of Ru.

Based on the observations of the microstructural stability of RR2100 and RR2101 at elevated temperature, the precipitation and growth of the TCP phases is clearly influenced by the presence of Ru in RR2101. Moderate levels of chemical heterogeneity retained within the microstructure after the solution heat treatment enable the TCP phases to nucleate continuously during the isothermal exposure. Hence, meaningful measurements of the corresponding TCP aspect ratios are difficult to obtain and interpret because the coarsening kinetics vary from precipitate to precipitate. Once the TCP phases nucleate within the dendritic cores, growth of the incoherent regions of the interface and propagation of the rod- or platelike structures into the interdendritic regions of the microstructure is primarily limited by diffusion of refractory elements such as W and Re to the TCP phases. The rate at which the TCP phases were able to percolate from the dendritic to interdendritic regions varied in the two nominally identical alloys with and without additions of 2 wt pct Ru. Isolated TCP phases were present in RR2100 immediately after primary aging, prior to the isothermal exposure (Figure 1(a)). After 1000 hours at 1100 °C, TCP precipitates were uniformly distributed throughout the microstructure (Figure 2(c)). Alloy RR2101 exhibited no TCP phases prior to aging (Figure 1(b)), and the onset of precipitation occurred after 400 hours at 1100 °C (Figure 2(b)). Compared to the degree of microstructural phase stability exhibited by RR2100, proliferation of the TCP phases into the interdendritic regions of the microstructure in RR2101 was extremely sluggish and did not occur until after 2000 hours at 1100 °C (Figure 2(d)). These observations may partially be explained by the destabilization of γ' associated with the presence of Ru. The Ru addition to alloy RR2101 modestly lowered the γ' solvus temperature[25] and decreased the overall fraction of γ' at elevated temperatures (Table III). Because the solubility of Re in the ordered γ' phase is inherently low, the decrease in the γ' volume fraction at elevated temperature corresponds to a decrease in the level of Re supersaturation in the γ phase. The increased fraction of γ phase in the Ru-bearing alloys at elevated temperatures accommodates higher concentrations of Re, Mo, and Cr without compromising microstructural stability and alleviating excess saturation *via* the precipitation and growth of TCP phases.

In the polycrystalline specimens, growth of cellular precipitates along the high-angle grain boundaries was not noticeably hindered by the presence of Ru in RR2101. Interestingly, for both alloys, TCP phases were revealed to nucleate readily along grain boundaries after only 90 minutes at 1180 °C and form lamellar structures during the progression of cellular precipitation. Since the mobility of the cellular precipitate interfaces are directly related to the diffusivity of Re along the boundaries,[26] the degree to which the cellular precipitates coarsened was not adversely affected by the presence of Ru. These observations are consistent with predictions from thermodynamic calculations that tend to suggest that Ru does not impact the microstructural stability of Ni-base superalloys at elevated temperatures.[27]

Compositional analysis of the TCP phases (Table IV) present in RR2101 revealed limited solubility of Ru within the various TCP phases. This is interesting since elemental Re and Ru possess the same crystal structure and are mutually soluble in one another. Because the kinetics of the diffusion-controlled precipitation reactions are generally limited by the slowest diffusing atomic species, the diffusivity of Re and Ru needs to be considered. Due to the high concentration of Re and W in the TCP phases, growth of these phases is likely to be limited by the diffusion of the element with the lowest mobility, Re, to the incoherent interfaces. Measurement of bulk diffusion coefficients in binary Ni-Ru and Ni-Re[24,28] and ternary Ni-Ru-Re[24] systems indicates that the diffusion of Re is approximately one order of magnitude lower than that of Ru at 1100 °C.[28] Exhibiting a higher diffusivity than Re, the transport of Ru away from the growing TCP or cellular precipitate interface is unlikely to inhibit the mobility of the incoherent TCP interfaces. However, elemental interactions and subtle changes in the character of the metallic bonding may impact interfacial partitioning characteristics in a manner that reduces the growth rate of the TCP phases.

Despite the similarity in crystal structure and chemical composition, the most notable differences between the TCP phases present in RR2100 and RR2101 is the marked differences in the precipitate coarsening rates. Because the

Table IV. Measured Volume Fraction of γ' at Various Temperatures; a Minimum of Eight Images Representative of Both the Dendritic and Interdendritic Regions Were Analyzed and Used to Assess the Errors

Temperature (°C)	Volume Fraction of γ' in RR2100 (Pct)	Volume Fraction of γ' in RR2101 (Pct)
25	76.3 ± 2	75.8 ± 2
900	74.8 ± 4	73.4 ± 4
1000	72.3 ± 5	67.6 ± 5
1100	55.3 ± 8	45.1 ± 8
γ' solvus temperature	1299 °C	1287 °C

TCP precipitates in RR2100 grow during the isothermal exposure at 1100 °C, the rod- or platelike morphologies gradually coarsen. Thickening of the precipitates corresponds with the depletion of Re and W from the adjacent γ phase. This leads to the eventual formation of an γ' envelope surrounding the TCP precipitate (Figure 4(a)). Even after 2000 hours at 1100 °C, the morphology of the TCP phases in RR2101 remained relatively unchanged as no significant thickening of the TCP precipitates was noted (Figure 4(d)). Coarsening of these refractory-rich TCP phases is dependent upon both the diffusion of solute to the mobile growth ledges and the continual nucleation of the growth ledges along the semicoherent interfaces. However, based on the results from this study, the presence of Ru appears to influence a number of different properties and cumulatively suppress the precipitation and growth of TCP phases at elevated temperatures. The degree of interfacial constraint imposed by the lattice mismatch between the TCP/γ-γ' interface, the interfacial partitioning associated with the intrinsically low solubility of Ru in the TCP precipitates, and the destabilizing effect Ru has on the γ' phase at elevated temperature all contribute to the enhancement of the overall stability of the microstructure.

In summary, the results from the present investigation clearly demonstrate that Ru additions are effective in minimizing the formation of TCP phases in high-refractory content single-crystal Ni-base superalloys during long-term isothermal exposures at elevated temperatures. Despite minimal changes in the characteristic chemical partitioning behavior between the constituent γ and γ' phases, significant differences in phase stability were observed. Due to the complexity of the multicomponent alloy systems, quantitatively isolating the mechanism(s) by which Ru suppresses TCP formation is extremely difficult. However, assessing the influence of Ru on the kinetics and thermodynamics individually may be possible *via* systematic changes on alloy composition. Finally, it is worth noting that the resulting improvements in microstructural stability due to Ru additions are extremely promising because they enable the development of creep-resistant single-crystal alloys amenable for use in extreme environments.

V. CONCLUSIONS

1. Additions of Ru greatly enhance the microstructural stability of high refractory content Ni-base single-crystal superalloys. After 1000 hours at 1100 °C, significant growth and coarsening of the TCP precipitates led to depletion of W and Re from the parent microstructure in RR2100. Although TCP phases were observed to form throughout the microstructure in the Ru-bearing alloy RR2101, growth of these phases was extremely limited and did not lead to significant depletion of refractory elements from the surrounding matrix.
2. Comparison of the isothermal phase stability of the two experimental alloys reveals that the rate at which TCP phases were able to effectively percolate from the dendritic to interdendritic regions decreased in the presence of Ru. The coarsening kinetics of the TCP phases in RR2101 were also influenced by the Ru addition as the size and morphology of the precipitates remained extremely fine even after prolonged elevated temperature exposures.
3. Re-rich σ- and *P*-phase precipitates were observed in both RR2100 and RR2101. Chemical analysis of the TCP phases in RR2101, however, revealed an extremely limited solubility of Ru within the precipitate.
4. Discontinuous cellular precipitation occurred along high-angle grain boundaries in both RR2100 and RR2101. The average fractions of the constituent phases in the cellular colonies (γ and TCP lamellae distributed within a γ' matrix) for both the Ru and non-Ru-bearing alloy were similar.

REFERENCES

1. W.S. Walston, K.S. O'Hara, E.W. Ross, T.M. Pollock, and W.H. Murphy: *Superalloys 1996*, TMS, Warrendale, PA, 1996, pp. 27-34.
2. S. Walston, A. Cetel, R. MacKay, K. O'Hara, D. Duhl, and R. Dreshfield: *Superalloys 2004*, Warrendale, PA, 2004, pp. 15-25.
3. J.X. Zhang, T. Murakamo, Y. Koizumi, T. Kobayashi, and H. Harada: *Acta Mater.*, 2003, vol. 51, pp. 5073-81.
4. G.L. Erickson: *Superalloys 1996*, TMS, Warrendale, PA, 1996, pp. 35-44.
5. P. Caron: *Superalloys 2000*, TMS, Warrendale, PA, 2000, pp. 737-46.
6. R. Darolia, D.F. Lahrman, and R.D. Field: *Superalloys 1988*, TMS, Warrendale, PA, 1988, pp. 255-64.
7. C.M.F. Rae, M.S.A. Karunaratne, C.J. Small, R.W. Broomfield, C.N. Jones, and R.C. Reed: *Superalloys 2000*, TMS, Warrendale, PA, 2000, pp. 767-76.
8. C.M.F. Rae and R.C. Reed: *Acta Mater.*, 2001, vol. 49, pp. 4113-25.
9. T.M. Pollock: *Mater. Sci. Eng.*, 1995, vol. B32, pp. 255-66.
10. O. Lavigne, C. Ramusat, S. Drawin, P. Caron, D. Boivin, and J.L. Pouchou: *Superalloys*, TMS, Warrendale, PA, 2004, pp. 667-76.
11. A.C. Yeh, C.M.F. Rae, and S. Tin: *Superalloys*, TMS, Warrendale, PA, 2004, pp. 677-86.
12. S. Tin and T.M. Pollock: *Mater. Sci. Eng.*, 2003, vol. A384, pp. 111-21.
13. A.C. Yeh and S. Tin: *Scripta Mater.*, 2005, vol. 52 (6), pp. 519-24.
14. K. O'Hara, W.S. Walston, E.W. Ross, and R. Darolia: U.S. Patent 5,482,789, 1996.
15. R.C. Reed, A.C. Yeh, S. Tin, S.S. Babu, and M.K. Miller: *Scripta Mater.*, 2004, vol. 51, pp. 327-31.
16. S. Tin, A.C. Yeh, A.P. Ofori, R.C. Reed, S.S. Babu, and M.K. Miller: *Superalloys*, TMS, Warrendale, PA, 2004, pp. 735-42.
17. A. Volek, F. Pycazk, R.F. Singer, and H. Mughrabi: *Scripta Mater.*, 2005, vol. 52, pp. 141-45.
18. T. Yokogawa, M. Osawa, K. Nishida, T. Kobayashi, Y. Koizumi, and H. Harada: *Scripta Mater.*, 2003, vol. 49, pp. 1041-46.
19. S. Tin, T.M. Pollock, and W. Murphy: *Metall. Mater. Trans. A*, 2001, vol. 32A, pp. 1743-53.
20. M.N. Gungor: *Metall. Trans. A*, 1989, vol. 20A, pp. 2529-33.
21. S. Tin, T.M. Pollock, and W.T. King: *Superalloys 2000*, TMS, Warrendale, PA, 2000, pp. 201-10.
22. T.M. Pollock, W.H. Murphy, E.H. Goldman, D.L. Uram, and J.S. Tu: *Superalloys 1992*, TMS, Warrendale, PA, 1992, pp. 125-34.
23. T.M. Pollock and W.H. Murphy: *Metall. Mater. Trans. A*, 1996, vol. 27A, pp. 1081-94.
24. R.A. Hobbs: Ph.D. Thesis, University of Cambridge, Cambridge, United Kingdom, 2006.
25. A.C. Yeh and S. Tin: *Parsons 2003*, Institute of Metals, London, 2003, pp. 673-86.
26. J.D. Nystrom, T.M. Pollock, W.D. Murphy, and A. Garg: *Metall. Mater. Trans. A*, 1997, vol. 28A, pp. 2443-52.
27. A.C. Yeh: Ph.D. Thesis, University of Cambridge, Cambridge, United Kingdom, 2005.
28. M.S.A. Karunaratne and R.C. Reed: *Acta Mater.*, 2003, vol. 51, pp. 2905-14.